

Electronic Supplementary Information

N, S co-doped porous carbon with Co₉S₈ prepared by Co- FF-derived Co₃O₄ template: A bi-functional electrocatalyst for rechargeable zinc–air battery

Qihao Wu,^{‡a} Tao Xie,^{‡a} Li Zhang,^{*a,b} Hui Ding,^a Heju Gao,^a Jiahui Jiang,^a Guancheng Xu^{*a}

^a State Key Laboratory of Chemistry and Utilization of Carbon Based Energy Resources; College of Chemistry, Xinjiang University, Urumqi, 830046, Xinjiang, PR China.

^b College of Chemical Engineering, Xinjiang University, Urumqi, 830046, Xinjiang, PR China.

[‡] These authors contributed equally to this work.

* Corresponding author

E-mail: zhangli420@xju.edu.cn, xuguanchengxju@163.com

1 Materials characterization

The phase of samples were characterized by powder X-ray diffraction (PXRD, Bruker D8 advance diffractometer, Cu K α radiation, $\lambda=0.15405$ nm). And the morphological images of samples were acquired by scanning electron microscopy (SEM, Hitachi S-4800). The elemental content and distribution of the compounds were analyzed by X-ray energy dispersive spectroscopy (EDS) and elemental mapping (FE-SEM, Hitachi SU8010 microscope). The contents of ingredients were detected by X-ray photoelectron spectroscopy (XPS, Escalab 250 Xi, Thermo Fisher Scientific). The degree of graphitization of carbon matrix in the samples was characterized by Raman spectroscopy (Raman, Bruker Senterra R 200-L). The Components of samples were characterized by Fourier Transform Infrared Spectrometer (FT-IR, Bruker VERTEX 70 RAMI).

2 Electrochemical measurement

All electrochemical tests were all performed at room temperature in a standard three-electrode system using a CHI 760E electrochemical workstation. The Ag/AgCl or Hg/HgO electrode and graphite rod were used as the reference and counter electrode, respectively. All measured potential were converted to the reversible hydrogen electrode (RHE) scale according to the Nernst equation ($E_{RHE} = E_{Ag/AgCl \text{ or } Hg/HgO} + 0.059 \text{ pH} + E^{\theta}$).

2.1 Working electrode preparation

The working electrode was prepared as follows: 2.5 mg of the catalyst was firstly dispersed in a mixed solution (500 μ L) of water/ethanol/Nafion with a volume ratio of 12:12:1, and then sonicated for 1 h to form a uniform catalyst ink. Afterwards, 10 μ L of catalyst ink was loaded onto a glassy carbon electrode with a diameter of 5.0 mm. After drying at room temperature for 0.5 h, a working electrode was obtained.

2.2 Electrochemical test method of ORR

The electrocatalytic ORR performance evaluation was performed in a standard three-electrode cell. The electrochemical performance was tested using graphite rods as counter electrode, drop-coated catalyst GCE as working electrode, and Ag/AgCl as reference electrode using electrochemical workstation CHI760E. Cyclic voltammetry (CV) measurements were performed in N₂ or O₂-saturated 0.1 M KOH solutions with a potential range from 0 to 1.2 V at a scan rate of 50 mV s⁻¹. Linear sweep voltammetry (LSV) curves were recorded during the 1600 rpm rotating disk electrode test. The stability of the catalysts was assessed by chronoamperometry for 1600 rpm at 0.2 V.

The electron transfer number (n) was further obtained from LSV curves measured at various rotating speeds (400–2025 rpm), and calculated according to Equation (1) and (2).

$$\frac{1}{j} = \frac{1}{j_L} + \frac{1}{j_K} = \frac{1}{B\omega^{1/2}} + \frac{1}{j_K} \quad (1)$$

$$B = 0.2nFC_o(D_o)^{2/3}\nu^{-1/6} \quad (2)$$

And the kinetic current density (j_K) was also calculated from equation (3).

$$j_K = \frac{j_L \times j}{j_L - j} \quad (3)$$

Where j and j_L is the measured and diffusion-limited current densities (mA cm⁻²), respectively. ω is the electrode rotating speed (rpm). B is the reciprocal of the slope determined from the Koutecky–Levitch (K–L) plots, and n is the number of electrons transferred per oxygen molecule. F is the Faraday constant (96485 C mol⁻¹); C_o is the concentration of O₂ (1.2×10^{-6} mol cm⁻³) in solution; ν is the kinetic viscosity (0.01 cm² s⁻¹), and D_o is the diffusion coefficient of O₂ in 0.1 M KOH (1.9×10^{-5} cm² s⁻¹).

The n and H_2O_2 yield for catalysts were examined by rotating ring-disk electrode techniques and calculated according to equation (4) and (5).

$$H_2O_2(\%) = 200 \times \frac{I_R/N}{I_D + I_R/N} \quad (4)$$

$$n = 4 \times \frac{I_D}{I_D + I_R/N} \quad (5)$$

Here, I_D and I_R are the disk and ring currents, respectively, and N (~ 0.47) is the current collection efficiency of the Pt ring.

2.3 Electrochemical test method of OER

The electrocatalytic OER performance evaluation was performed in a standard three-electrode cell. The electrochemical performance was tested using graphite rods as counter electrode, drop-coated catalyst GCE as working electrode, and Hg/HgO as reference electrode using electrochemical workstation CHI760E. LSV curves were obtained in 1 M KOH solution at a scan rate of 5 mV s^{-1} over a voltage range of 1.0 to 1.8 V. The electrochemical AC impedance spectra (EIS) were obtained using an AC current of 5 mV in the frequency range of 100000 to 0.1 hz, tested at voltages corresponding to a current density of 10 mA cm^{-2} . The bilayer capacity (C_{dl}) was used to measure the electrocatalytic surface active area of the catalyst. The CV curves of the catalysts were tested in 1 M KOH solution at different sweep rates (20, 40, 60, 80, 100 mV s^{-1}) in the potential range of 0.97–1.07 V, and C_{dl} calculated from equation (6).

$$C_{dl} = \frac{i}{v} \quad (6)$$

where i is the current density and v is the sweep speed.

2.4 Assembly and testing of ZAB

The zinc–air battery (ZAB) was tested in an electrolyte solution containing 6 M KOH and 0.2 M $\text{Zn}(\text{CH}_3\text{COO})_2$, zinc foil was used as the anode, and the air cathode was made from commercial carbon paper (P₂, Changsha Spring New Energy Technology Co., Ltd.) coated with catalysts ($\text{Co}_9\text{S}_8/\text{NSC}$ or Pt/ C and RuO_2) ink (loading capacity is 1 mg cm⁻²). All tests were carried out in CHI 760E. The specific capacity was calculated and normalized by using the amount of consumed Zn during discharge.

3 Figures

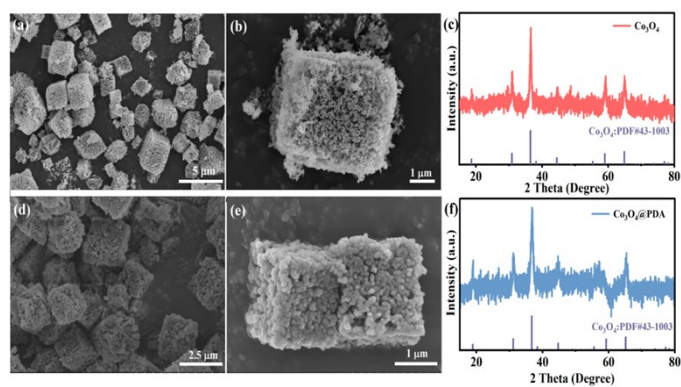


Fig. S1 (a, b) SEM images and (c) XRD pattern of Co_3O_4 . (d, e) SEM images and (f) XRD pattern of Co_3O_4 @PDA.

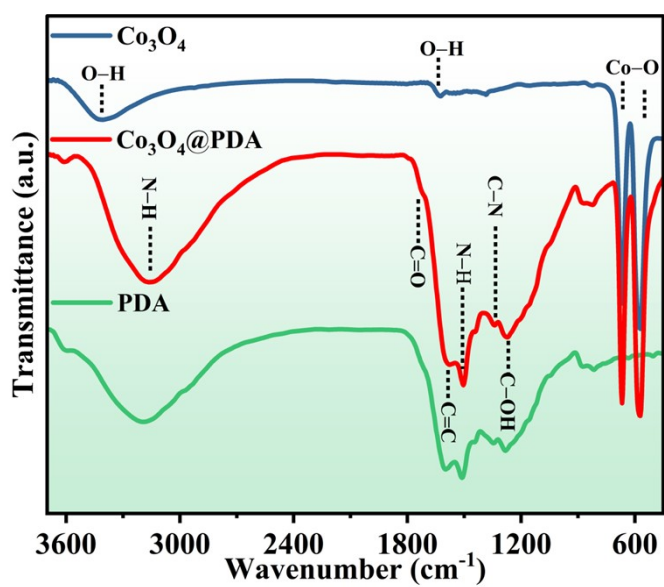


Fig. S2 FT-IR spectra of Co_3O_4 , Co_3O_4 @PDA and PDA.

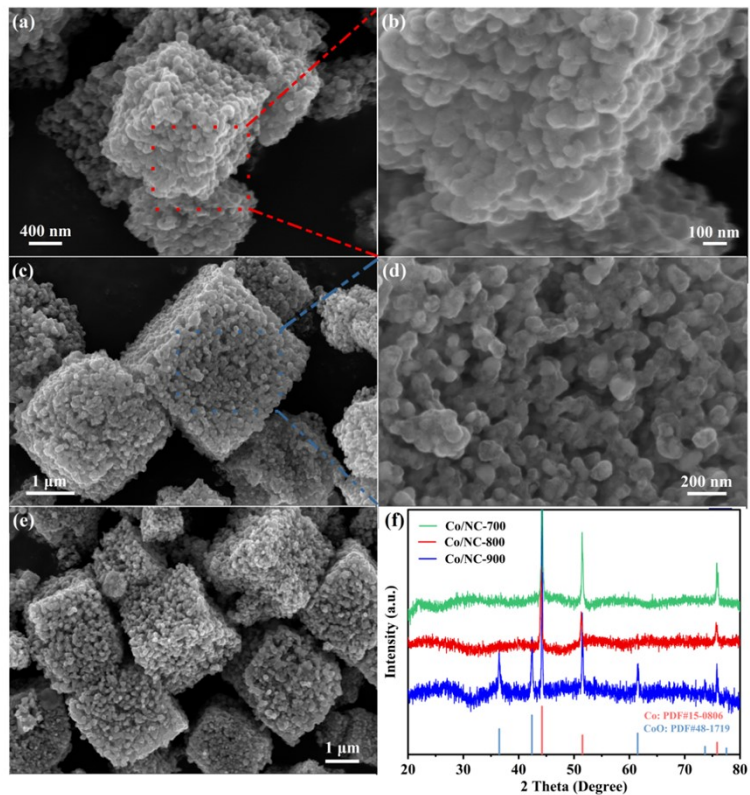


Fig. S3 SEM images of (a, b) Co/NC-800, (c, d) Co/NC-700 and (e) Co/NC-900. (f) PXRD patterns of the different samples.

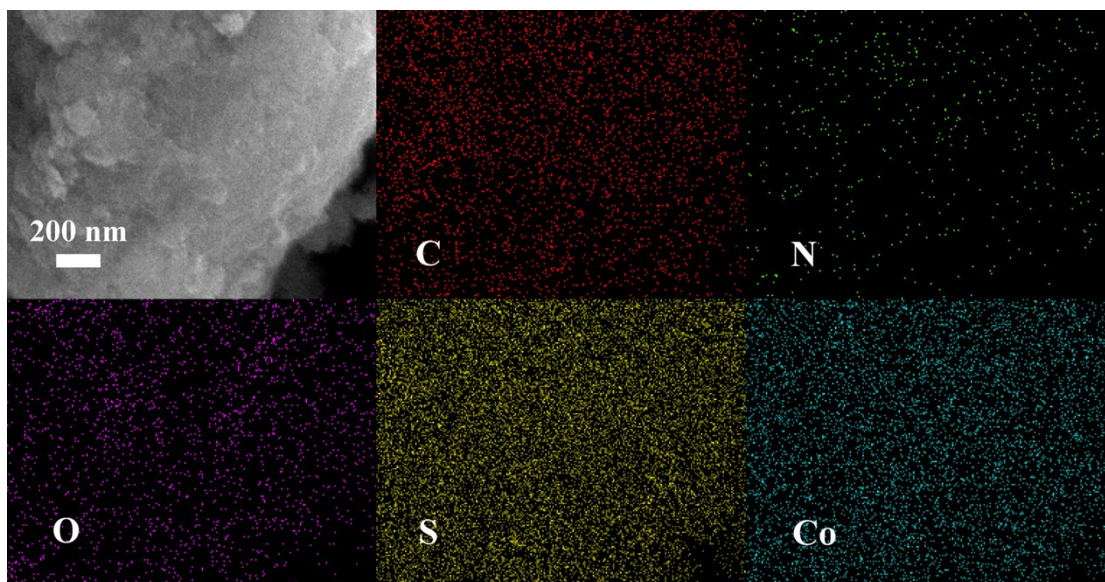


Fig. S4 Element mapping images of Co₉S₈/NSC-1.

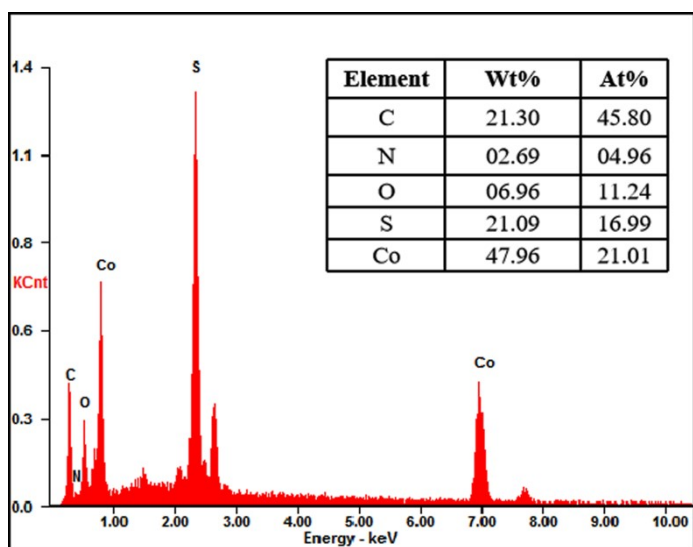


Fig. S5 EDS spectrum of $\text{Co}_9\text{S}_8/\text{NSC-1}$.

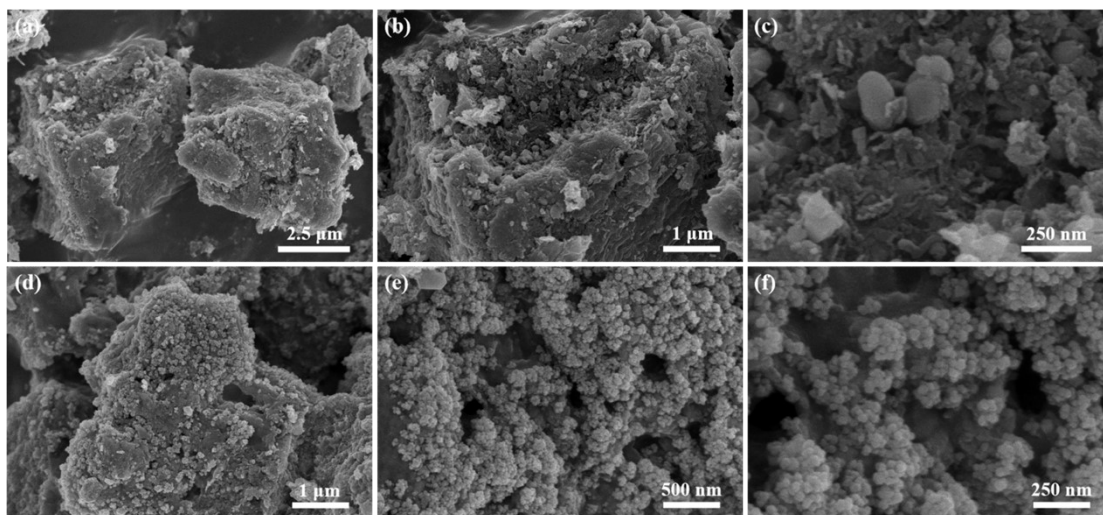


Fig. S6 SEM images of (a–c) $\text{Co}_9\text{S}_8/\text{NSC-2}$ and (d–f) $\text{Co}_9\text{S}_8/\text{NSC-3}$.

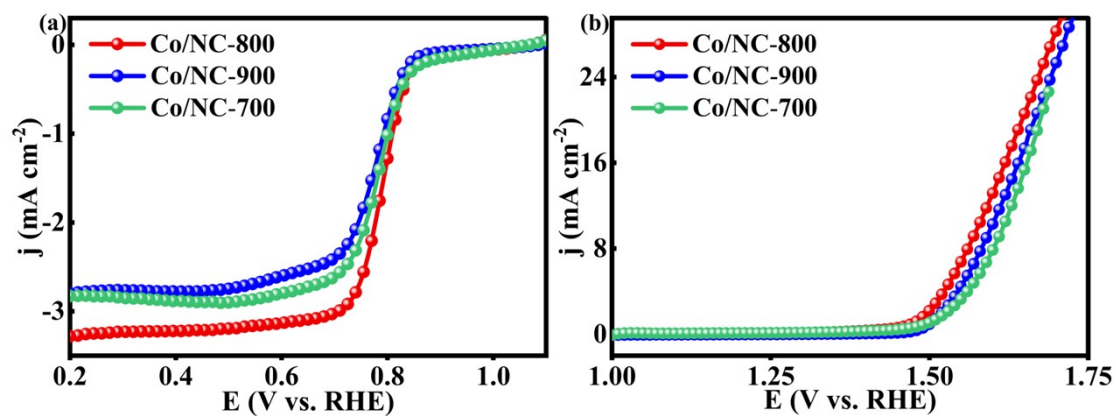


Fig. S7 LSV curves of (a) ORR and (b) OER for the different samples.

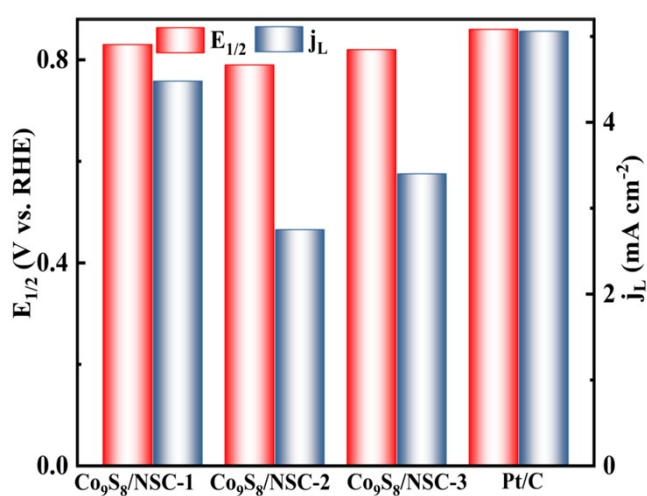


Fig. S8 $E_{1/2}$ and j_L of the catalysts.

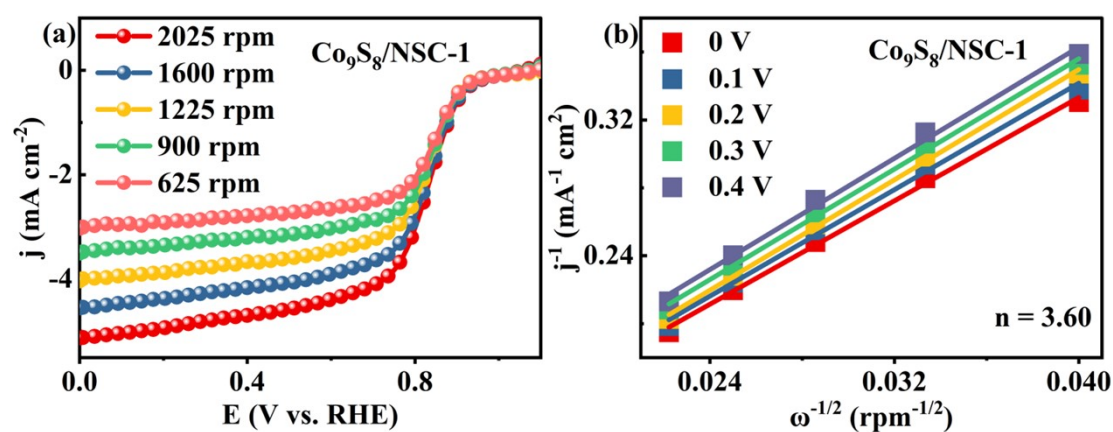


Fig. S9 (a) LSV curves at different rotational speeds (from 625 to 2025 rpm) and (b) fitted K-L plots of Co₉S₈/NSC-1.

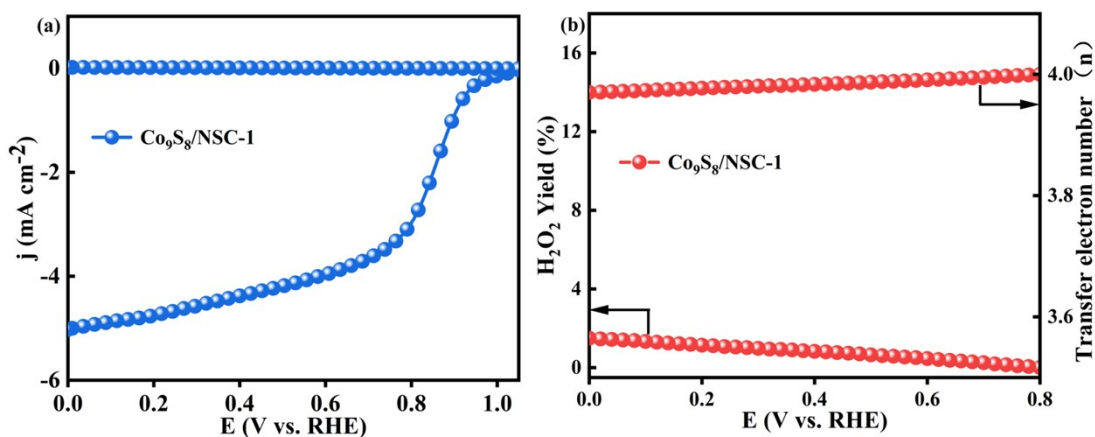


Fig. S10 (a) LSV curve and (b) Electron transfer number and H₂O₂ yield of Co₉S₈/NSC-1.

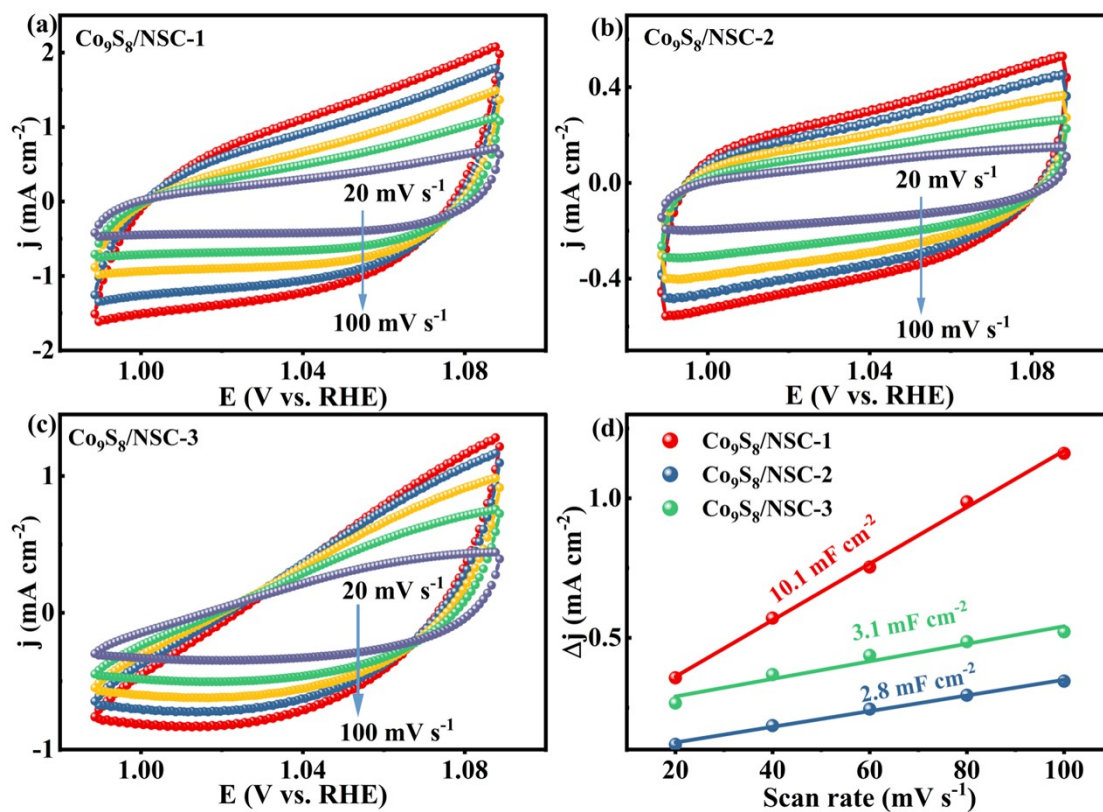


Fig. S11 CV curves of (a) Co₉S₈/NSC-1, (b) Co₉S₈/NSC-2 and (c) Co₉S₈/NSC-3 at different sweep rates (from 20 to 100 mV s⁻¹). (d) Calculated electrochemical double-layer capacitance (C_{dl})

in the non-faradaic region for the samples.

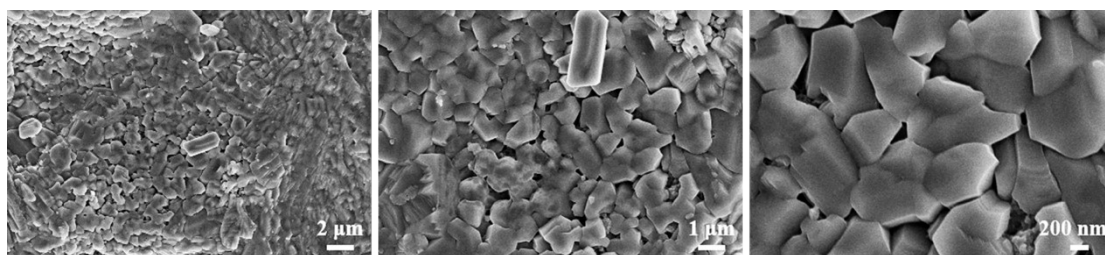


Fig. S12 SEM images of the Co₉S₈/NSC-1 after 500 charge/discharge cycles.

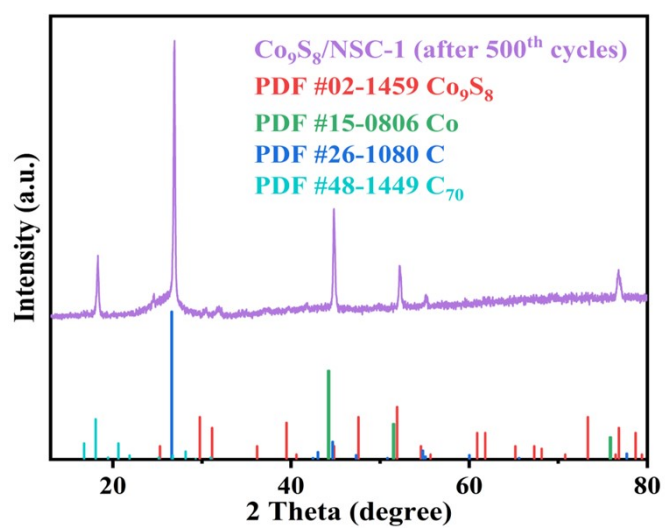


Fig. S13 XRD pattern of Co₉S₈/NSC-1 after cycling test in aqueous zinc-air battery.

4 Table

Table S1 Comparison of electrocatalytic activity of the Co₉S₈/NSC-1 with recently reported ORR/OER bifunctional oxygen electrode materials.

Electrocatalysts	E_{j=10} (V vs. RHE)	E_{1/2} (V vs. RHE)	ΔE (V)	maximum power density (mW cm⁻²)	Cycle life (h)	Ref.
Co ₉ S ₈ /NSC-1	1.53	0.83	0.70	102.0	167	This work
Co/Co ₉ S ₈ @SNC-900	1.54	0.82	0.72	106.6	107	[1]
Co ₉ S ₈ /Co _{1-x} S@NSC	1.52	0.86	0.66	141.9	70	[2]
Co ₉ S ₈ /CoNSC-900	1.57	0.89	0.68	150	40	[3]
Co ₉ S ₈ -HCT	1.46	0.86	0.60	146	60	[4]
Zn _{0.76} Co _{0.24} SeCo ₉ S ₈	1.56	0.83	0.73	—	—	[5]
Co ₉ S ₈ @Co/Mn-S ₂ N-PC	1.55	0.85	0.70	80	210	[6]
Co-IM-POP-1000	1.70	0.79	0.91	234	260	[7]
Co ₉ S ₈ @NSC	—	0.85	—	150.9	—	[8]
Co ₉ S ₈ /NSC-3	1.58	0.82	0.76	85	140	[9]
Cu-Co ₉ S ₈ -NHCS-1	1.56	0.77	0.79	91	120	[10]

References

1. Y. Zhang, J. Ma, M. Ma, C. Zhang, X. Jia and G. Wang, *J. Mater. Res. Technol.*, 2022, **18**, 3764–3776.
2. C. Sun, J. Ding, H. Wang, J. Liu, X. Han, Y. Deng, C. Zhong and W. Hu, *J. Mater. Chem. A*, 2021, **9**, 13926–13935.
3. J. Zhang, B. Cui, S. Jiang, H. Liu and M. Dou, *Nanoscale*, 2022, **14**, 9849–9859.
4. J. Zhao, J. Zhou, Z. Zhang, Q. Li and R. Liu, *Chem. Eng. J.*, 2021, **418**, 129365.
5. P. Yang, F. Kong, X. Sui, L. Zhao, Y. Qiu, H. Zhang and Z. Wang, *Int. J. Hydrogen Energy*, 2022, **47**, 8811–8819.
6. R. M. Sun, L. Zhang, J. J. Feng, K. M. Fang and A. J. Wang, *J. Colloid. Interface Sci.*, 2022, **608**, 2100–2110.
7. H. Luo, X. Chen, T. Huang, W. Kang, X. Li, Z. Jiang, L. Pang, J. Bai, W. Tan, J. Li and B. Zhou, *J. Environ. Chem. Eng.*, 2022, **10**, 107203.
8. T. Yu, Y. Che, H. Fu, D. Ma, W. Zhao, S. Yan, T. Bian and L. Zhang, *J. Alloys Compd.*, 2023, **948**, 169792.
9. Y. Peng, F. Zhang, Y. Zhang, X. Luo, L. Chen and Y. Shi, *Dalton Trans.*, 2022, **51**, 12630–12640.
10. Y. Xie, S. J. Li, J. P. Huang, R. Qiu, Z. Q. Liu and N. Li, *J. Alloys Compd.*, 2022, **921**, 166076.